

Graphene-NiO Nanohybrid Prepared by Dry Plasma Reduction as a Low-cost Counter Electrode Material for Dye-sensitized Solar Cells

Van-Duong Dao^a, Liudmila L. Larina^{a,b}, Kwang-Deog Jung^c, Joong-Kee Lee^d, Ho-Suk Choi^{a*}

^a*Department of Chemical Engineering, Chungnam National University, 220 Gung-Dong,
Yuseong-Gu, Daejeon 305-764, Korea*

^b*Institute of Biochemical Physics, Russian Academy of Sciences, Kosygin St. 4, 119334 Moscow,
Russia*

^c*Clean Energy Research Center, Korea Institute of Science and Technology, P.O. Box 131,
Cheongryang, Seoul 130-650, Korea*

^d*Energy Storage Research Center, Korea Institute of Science and Technology, P.O. Box 131,
Cheongryang, Seoul 130-650, Korea*

(* Corresponding Author: hchoi@cnu.ac.kr)

Preparation of TiO₂ working electrodes

We fabricated the DSC working electrode coated with TiO₂ layer of 0.7 cm x 0.7 cm on the FTO glass of 2 cm x 2 cm through the following procedure. The substrates were first cleaned in an acetone (Fluka) using an ultrasonic bath for 30 min. After cleaning, the substrates were immersed in a 40 mM aqueous TiCl₄ solution at 70 °C for 30 min and washed with water and ethanol. A transparent film of 20 nm TiO₂ particles (Solaronix, Switzerland) was coated on the substrates by screen printing (200 T mesh), kept in a clean box for 3 min so that the paste could relax to reduce the surface irregularity and then dried for 3 min at 125 °C. This screen-printing procedure (coating, storing, and drying) was repeated to the thickness of the working electrode of around 12 µm. We then also coated a 4 µm thick scattering layer of TiO₂ paste (DSL 18 NR-AO, Dyesol-Timo, Australia) on a working electrode [S1]. The electrodes coated with the TiO₂ pastes were gradually heated under air flow at 325 °C for 5 min, at 375 °C for 5 min, at 450 °C for 15min, and finally at 500 °C for 15 min under ambient condition. After annealing, the TiO₂ film was treated with 40 mM TiCl₄ solution as described above, and sintered at 500 °C for 30 min [S1]. After cooling down to 80 °C, the TiO₂ electrodes were immersed in a 0.3 mM N719 dye

solution in a mixture of acetonitrile (Sigma-Aldrich) and tert-butyl alcohol (Aldrich) (volume ratio of 1:1) and kept at room temperature for 24 h to complete the sensitizer uptake.

Assembly of DSCs

The dye-covered TiO₂ electrode and counter electrodes were assembled onto a sandwich type cell and sealed at 120 °C for 5 min with a thermobonding polymer (Surlyn, DuPont) of 60µm thickness. A drop of the electrolyte, a solution of 1-methyl-3-butylimidazolium iodide (Sigma-Aldrich), 0.03 M I₂ (Sigma-Aldrich), 0.10 M guanidinium thiocyanate (Sigma-Aldrich), and 0.50 M 4-tert-butylpyridine (Aldrich) in mixed solvent of acetonitrile (Sigma-Aldrich), and valeronitrile (volume ratio of 85:15) was placed on the hole (0.8 mm) in the back of the working electrode. The holes were sealed with a Surlyn layer [S1].

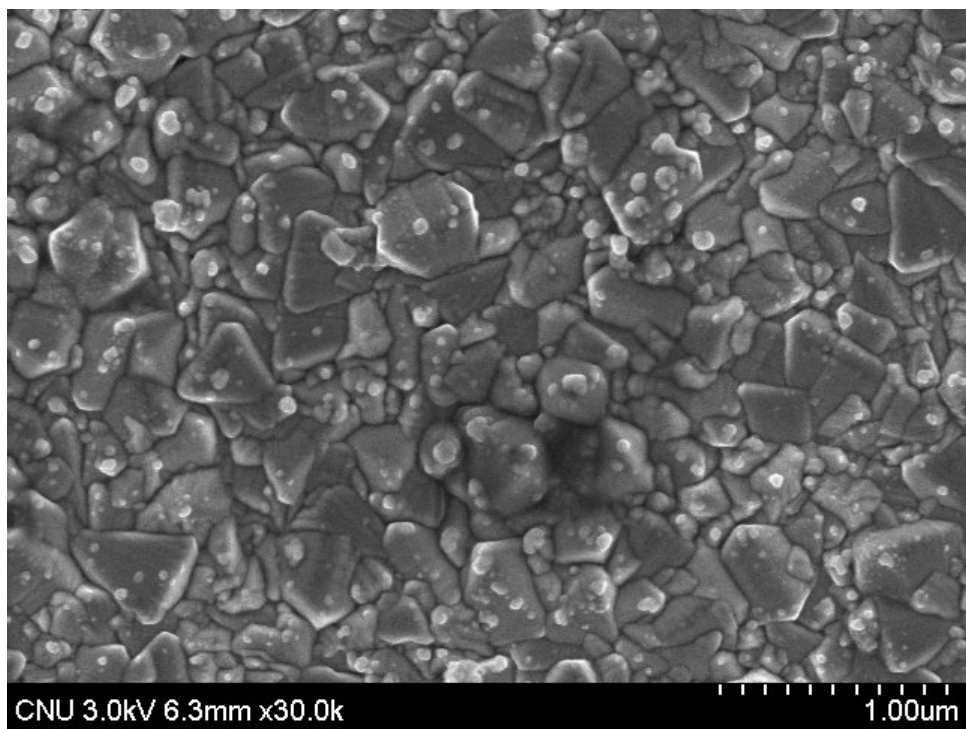


Figure S1. SEM of NiO-NPs directly immobilized on FTO glass by means of dry plasma reduction

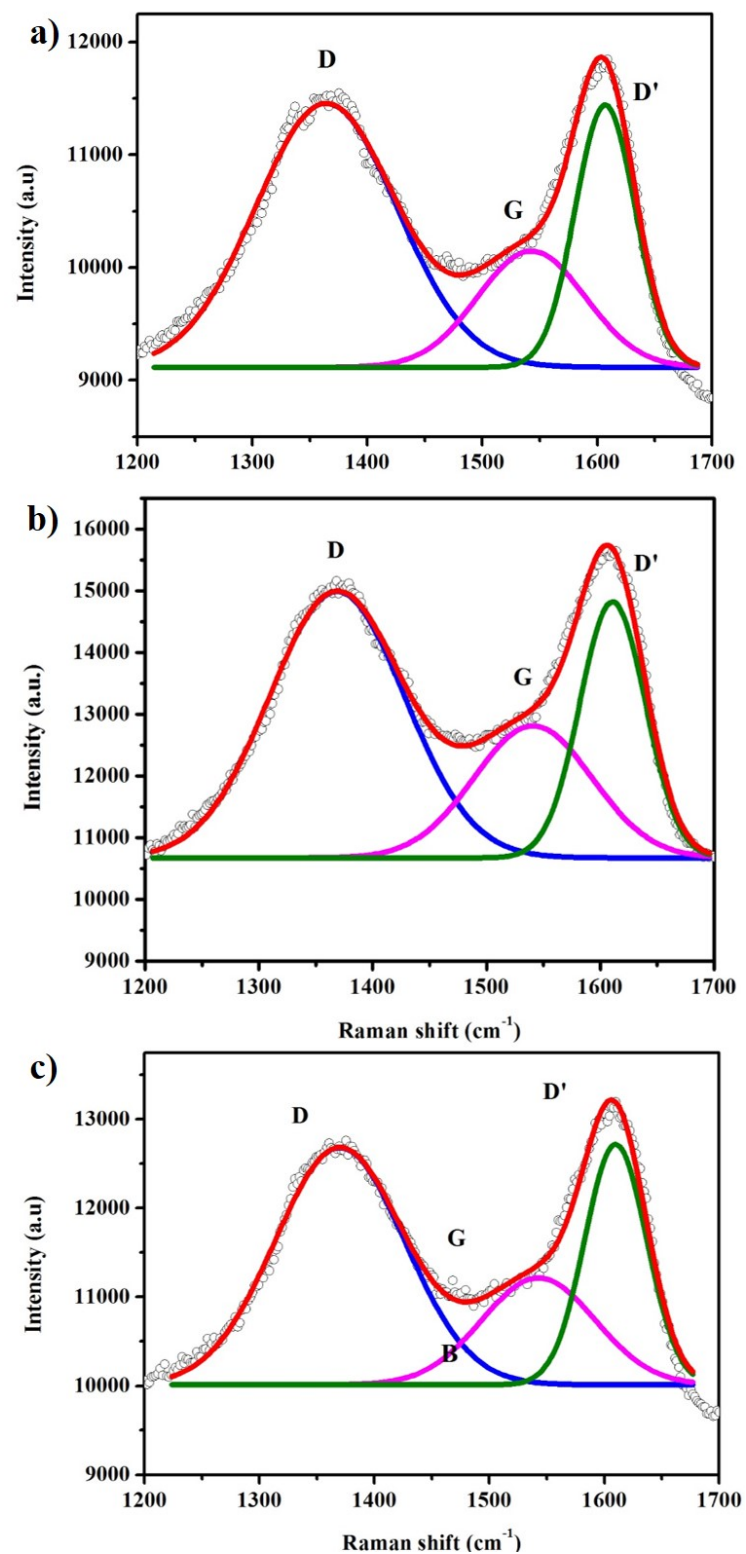


Figure S2. Raman spectra of the GO (a), RGO (b) and NiO-NP/RGO nanohybrid (c)

Redox behavior of NiO-NP/RGO nanohybrid materials

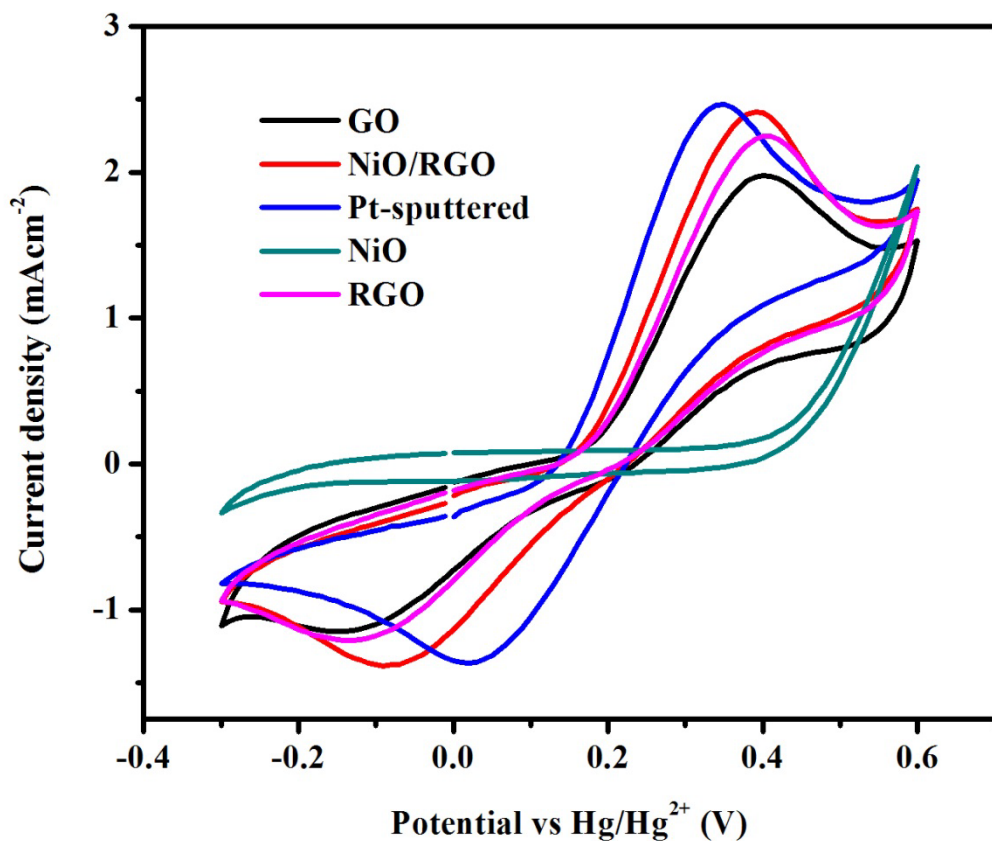


Figure S3. Cyclic voltammograms of Pt-sputtered, NiO-NP/RGO nanohybrid-coated, GO-coated, RGO-coated, and NiO-NP-immobilized electrodes

The catalytic performances of Pt-sputtered, NiO-NP/RGO nanohybrid-coated, GO-coated, RGO-coated, NiO-NP-immobilized electrodes were evaluated through a comparative analysis of the cyclic voltammograms (CV) of these five electrodes in a 5 mM LiI + I₂ acetonitrile solution containing 0.1 M LiClO₄ as the supporting electrolyte [S1]. For cyclic voltammetry, the five electrodes were used as working electrodes, the Pt mesh was a CE, and Hg/Hg²⁺ in acetonitrile served as a reference electrode. The data were recorded from 600 mV to -300 mV at a scan rate of 50 mV s⁻¹ [S1]. Figure S3 shows that the NiO-NP/RGO nanohybrid electrode exhibits a higher current density, as evidenced by the large peak area in the CV curve, suggesting a larger active surface [S1,S2]. While the reduction reaction of triiodide ions on the GO, RGO and NiO electrode is very slow, the NiO-NP/RGO nanohybrid electrode shows the highest cathodic peak,

indicating that it has high electro-catalytic activity. This high electro-catalytic activity can reduce the charge transfer resistance at the CE/electrolyte interface. This not only reduces internal resistance levels but also attenuates the recombination rates and concentration gradients in the electrolyte, which have been proved to affect the short-circuit current density (J_{sc}) strongly [S3].

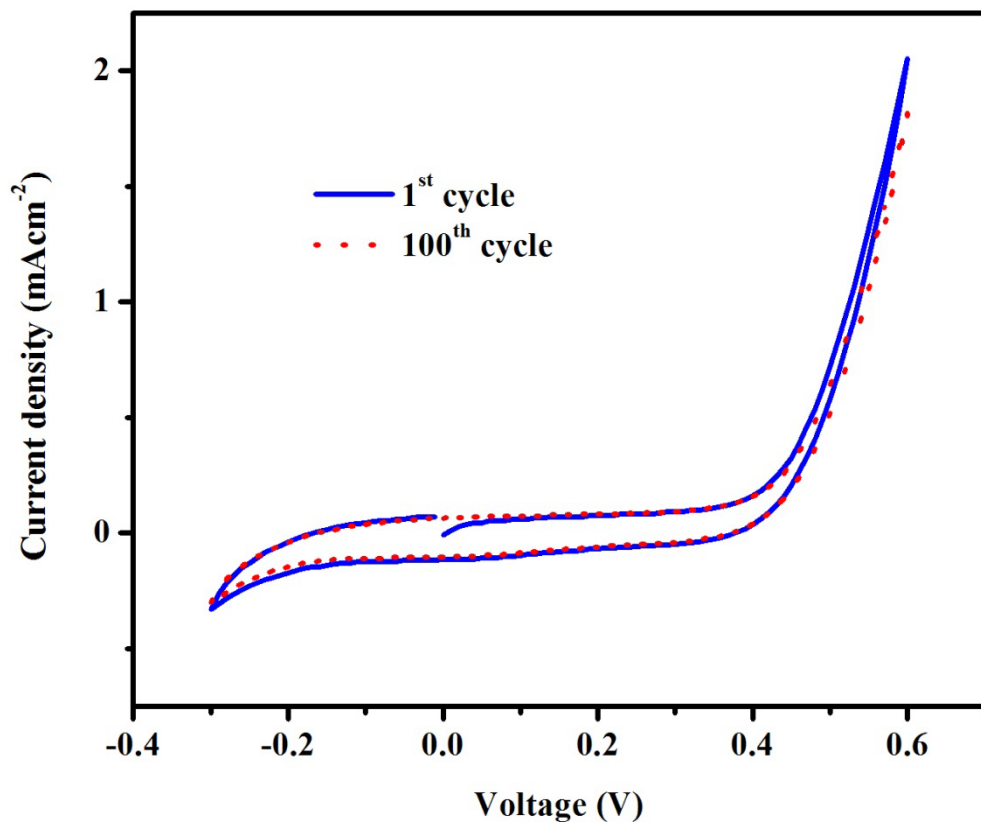


Figure S4. Current-voltage curves over time for the redox system with the NiO NPs working electrode prepared by dry plasma reduction and Pt-mesh counter electrode.

The stability of the electrode materials is very important for applications. The DSC with the NiO NP as counter electrode prepared by dry plasma reduction showed good stability. This stability was confirmed by the stability of the current-voltage curves over time for the redox system with the NiO NP working electrode and Pt mesh counter electrode (Figure S4) [S4]. Slight decrease of the current was observed after the 100th cycle. It is, however, better than that of Pt counter electrode prepared by thermal decomposition [S4].

The role of NiO-NPs as bridges to facilitate electron transport

The reduction of I_3^- to I^- at the interface between counter electrode (CE) and electrolyte takes place in three stages. The first is the diffusion and adsorption of I_3^- from bulk solution onto the surface of CE. The second is the reduction of I_3^- into I^- . The third is the desorption and diffusion of I^- from the surface of CE to the bulk electrolyte [S5]. The desorption rate of I^- from CE is naturally one of factors which limit the rate of the I_3^-/I^- redox process. The desorption rate of reduced I^- depends on various factors such as desorption energy [S6], CE surface structure [S7] and morphology [S8], CE roughness factor or the double layer thickness [S7]. Thus, the CE roughness increased due to hybridizing of NiO-NPs on RGO surface can result in the increase of thin double layer, compared with a thick double layer existing at the CE with a smooth surface of Pt-sputtered film [S9]. The double layer can also block the diffusion of iodide and triiodide ions near the electrode surface [S7]. Therefore, the increase of the CE roughness may facilitate the diffusion of I_3^- and I^- ions, and in turn, increase the rate of the I_3^-/I^- redox process.

The reduction of GO also results in the partial restoration of the sp^2 carbon-carbon bonds. Their distribution in the graphene lattice, however, does not induce an expansion of a continuous sp^2 domain. Usually 60% of the area contains graphitic domains with size in range of 3 to 10 nm. The clusters are isolated by the disordered structure (sp^3) of oxygen functional groups [S10]. Even the best reduction methods still yield the RGO with 8% oxygen functional groups. The disordered structure (sp^3) significantly hampered the carrier transport. Therefore, the electrical conductivity and mobility in RGO are not as high as in pristine graphene. An average trap density of $\sim 1.75 \times 10^{16} \text{ cm}^{-3}$ was found through the electron transport measurements [S11]. Given a lot of defects which localize charge carriers, the hopping transport mechanism in RGO, which explains the charge transfer via hopping among the localized states, was suggested [S12]. Both “Mott VRH” model and “Efros-Shklovskii VRH” model for hopping transport were proven [S13, S14]. Thus, we suggest that NiO hybridized on the surface of RGO can facilitate the electron conductivity of NiO-NP/RGO structure by providing the localized surface states for the hopping transport. Indeed, the surface states within the forbidden gap of NiO were identified by electron energy loss spectroscopy (EELS) [S15]. In an EEL spectrum, both the optically allowed transitions and spin-forbidden transitions can be observed [S15]. The mapping of the surface-state energy distribution with peak positions of 0.6, 1.1 and 1.8 eV for NiO was provided.

Therefore, in the NiO-NP/RGO structure, the localized states, identified as NiO surface states, can act as electron or hole traps, supporting the charge transfer (the hopping transport) among the localized states of RGO.

References

- [S1] V. D. Dao, S. H. Kim, H. S. Choi, J. H. Kim, H. O. Park, J. K. Lee, *J. Phys. Chem. C* 2011, **115**, 25529.
- [S2] G.-R. Li, F. Wang, Q.-W. Jiang, X.-P. Gao, P.-W. Shen, *Angew. Chem., Int. Ed.*, 2010, **122**, 3735.
- [S3] Z. Tachan, M. Shalom, I. Hod, S. Ruhle, S. Tirosh, A. Zaban, *J. Phys. Chem. C* 2011, **115**, 6162-6166.
- [S4] X. Mei, S. Cho, B. Fan and J. Ouyang, *Nanotechnology* 2010, **21**, 395202
- [S5] Y. Tang, X. Pan, C. Zhang, S. Dai, F. Kong, L. Hu, Y. Sui, *J. Phys. Chem. C* 2010, **114**, 4160-4167
- [S6] Y. Hou, D. Wang, X. H. Yang, W. Q. Wang, B. Zhang, H. F. Wang, G. Z. Lu, P. Hu, H. J. Zhao, H. G. Yang, *Nat. Commun* 2013, **4**, 1583
- [S7] T. L. Hsieh, H. W. Chen, C. W. Kung, C. C. Wang, R. Vittal, K. C. Ho, *J. Mater. Chem.*, 2012, **22**, 5550-5559
- [S8] S. Mukherjee, B. Ramalingam, L. Griggs, S. Hamm, G. A. Baker, P. Fraundorf, S. Sengupta and S. Gangopadhyay, *Nanotechnology* 2012, **23**, 485405.
- [S9] L. I. Daikhin, A. A. Kornyshev, M. Urbakh, *Electrochim. Acta* 1997, **42**, 2853-2860
- [S10] K. Erickson, R. Erni, Z. Lee, N. Alem, W. Gannett, A. Zettl, *Adv. Mater* 2010, **22**, 4467
- [S11] D. Joung, A. Chunder, L. Zhai, S. I. Khondaker, *Appl. Phys. Lett.*, 2010, **97**, 093105
- [S12] N. F. Mott, E. A. Davis, *Electronic processes in non-crystalline materials*. 2nd ed. Oxford (UK): Clarendon Press; 1979.

- [S13] A. B. Kaiser, C. Gomez-Navarro, R. S. Sundaram, M. Burghard, K. Kern, *Nano Lett* 2009, **9**, 1787
- [S14] D. Joung, L. Zhai, S. I. Khondaker, *Phys. Rev. B* 2011, **83**, 115323
- [S15] A. Freitag, V. Staemmler, D. Cappus, C.A. Ventrice Jr., K. Al Shamery, H. Kuhlenbeck, H.-J. Freund, *Chem. Phys. Lett.*, 1993, **210**, 10